doi:10.1006/jmbi.1999.3470 available online at http://www.idealibrary.com on IDEAL® J. Mol. Biol. (2000) 296, 1053–1063

JMB

Thermodynamics of DNA Binding and Condensation: Isothermal Titration Calorimetry and Electrostatic Mechanism

Daumantas Matulis†, Ioulia Rouzina and Victor A. Bloomfield*

Department of Biochemistry Molecular Biology and Biophysics, University of Minnesota, 1479 Gortner Avenue, St. Paul MN 55108, USA

*Corresponding author

The thermodynamics of binding of the trivalent cations cobalt hexammine and spermidine to plasmid DNA was studied by isothermal titration calorimetry. Two stages were observed in the course of titration, the first attributed to cation binding and the second to DNA condensation. A standard calorimetric data analysis was extended by applying an electrostatic binding model, which accounted for most of the observed data. Both the binding and condensation reactions were entropically driven ($T\Delta S \sim +10$ kcal/mol cation) and enthalpically opposed ($\Delta H \sim +1$ kcal/mol cation). As predicted from their relative sizes, the binding constants of the cations were indistinguishable, but cobalt hexammine had a much greater DNA condensing capacity because it is more compact than spermidine. The dependence of both the free energy of cobalt hexammine binding and the critical cobalt hexammine concentration for DNA condensation on temperature and monovalent cation concentration followed the electrostatic model quite precisely. The heat capacity changes of both stages were positive, perhaps reflecting both the temperature dependence of the dielectric constant of water and the burial of polar surfaces. DNA condensation occurred when about 67% of the DNA phosphate charge was neutralized by cobalt hexammine and 87% by spermidine. During condensation, the remaining DNA charge was neutralized.

© 2000 Academic Press

Keywords: DNA condensation by multivalent cations; electrostatics; polyelectrolyte; enthalpy of binding; cobaltic(III) hexammonium chloride; spermidine

Introduction

Multivalent cations like cobalt(III) hexammine and spermidine^{3+} bind to extended DNA double helices and condense them into compact, orderly particles. The phenomenon of DNA condensation by multivalent cations poses challenging physical puzzles, is biologically important as a model for viral DNA packaging and chromosome folding, and has potential biotechnological and medical interest as a key step in non-viral gene therapies. It has therefore been extensively studied by a variety of experimental techniques, and various physical mechanisms have been proposed to account for the attractive force driving condensation (for reviews, see Bloomfield, 1996, 1998). Direct measurements of the thermodynamic changes accompanying DNA condensation are needed to test and parameterize these theoretical proposals.

In very dilute solutions a striking toroidal morphology of the condensed DNA particles is observed, which has led to many studies of DNA condensation by light scattering, electron and scanning probe microscopy, and other techniques suitable for very low macromolecular concentrations (Bloomfield, 1996, 1998). Discrete condensed particles containing only one or a few DNA molecules will not be found at the higher DNA concentrations needed in studies of osmotic stress (Leikin *et al.*, 1991; Rau & Parsegian, 1992a,b) and liquid crystal (Pelta *et al.*, 1696; Raspaud *et al.*, 1998, 1999; Sikorav *et al.*, 1994) behavior, or in the calorimetric study reported here. Nevertheless, the fundamental

†On leave from Institute of Biochemistry, Mokslininku 12, 2600 Vilnius, Lithuania.

Abbreviations used: ITC, isothermal titration calorimetry.

E-mail address of the corresponding author: victor@tc.umn.edu

0022-2836/00/041053–11 $35.00/0 © 2000 Academic Press

intermolecular energetic factors responsible for condensation are probably the same regardless of DNA concentration, and higher DNA concentrations enable the high accuracy and precision of direct thermodynamic measurements which are impossible at high dilution. Here we report measurements of the energetics of multivalent cation binding and DNA condensation by isothermal titration calorimetry (ITC).

We determined the energetics of two consecutive processes, multivalent cation binding to DNA followed by DNA condensation, in a single isothermal titration calorimetry experiment. Thermodynamic parameters (Gibbs free energy, enthalpy, entropy, and heat capacity) of both processes were evaluated by applying standard methods of calorimetric data analysis. Interestingly, the entropically driven reaction was observed through a relatively small (~10 %) change in the enthalpy, which opposes the reaction. We developed a method for fitting the binding curves with an electrostatic anticooperative binding model (Rouzina & Bloomfield, 1996a, 1997), which accurately predicted the dependence of the free energies of both processes on monovalent cation concentration and temperature. Previous calorimetric studies have measured the thermodynamics of multivalent cations to DNA (Ross & Shapiro, 1974) and observed a two-stage process when singly charged cationic lipid binds to DNA (Spink & Chaires, 1997). Our work extends those studies by measuring binding and DNA condensation by multivalent cations and interpreting the results quantitatively using an electrostatic theory.

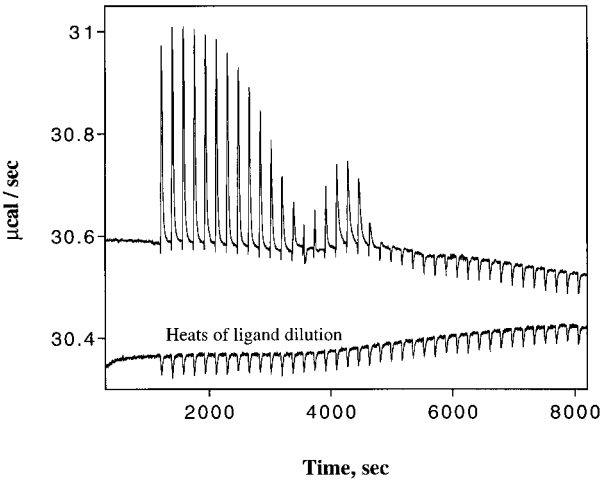

Figure 1. Representative calorimetric titration curves. The upper curve was obtained by titrating DNA with cobalt hexammine (10 mM NaCl in the cell and syringe). The lower curve was obtained with no DNA, showing the heats of dilution which were subtracted in order to obtain binding curves.

Results

Two stages of cobalt hexammine and spermidine binding to pUC118 DNA

Cobalt hexammine and spermidine binding to pUC118 plasmid DNA were studied by ITC. A typical experimental trace, and the heat of dilution trace which was subtracted therefrom (see Materials and Methods), are shown in Figure 1. The titration curves in 10 mM NaCl at 25 °C, shown in Figure 2, indicate that the cations bind to DNA in two stages. Standard analysis (see below) of calorimetric data showed that during the first stage, DNA bound an amount of cobalt hexammine sufficent to neutralize only about two-thirds of the negative charge on DNA. Small further additions of the cation did not evolve additional enthalpy. At a critical concentration of cobalt hexammine, a second enthalpic peak occured. During this second stage of binding an additional amount of the negative charge on DNA was neutralized to a total of 85-90 % (Widom & Baldwin, 1980; Wilson & Bloomfield, 1979), the reaction of DNA condensation and aggregation occurred, and increased turbidity of the solution could be observed visually. The enthalpies, entropies, and association constants for both stages were similar and are listed in Tables 1 and 2.

Spermidine is a weaker condensing agent than cobalt hexammine (Widom & Baldwin, 1980, 1983). As seen in Figure 2, it took more spermidine than cobalt hexammine to reach the second stage of aggregation. However, the first stages of both ligand binding curves were indistinguishable. Integral enthalpies of first-stage binding per mole

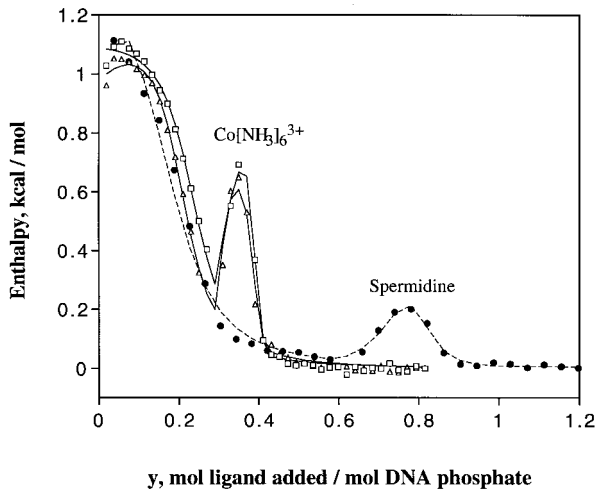

Figure 2. Isothermal titration calorimetric curves of cobalt hexammine (open symbols, continuous line) and spermidine (●, dashed line) binding to pUC118 DNA at 10 mM NaCl and 25 °C. Peaks corresponding to two stages are seen: initial binding and aggregation. No significant difference is observed between circular pUC118 plasmid (△) and linearized pUC118 plasmid (□), digested with *Sma*I restriction enzyme on a single site.

Table 1. Thermodynamic parameters per mole of cobalt hexammine and spermidine binding to pUC118 plasmid DNA in the first stage as determined by ITC

[NaCl] (mM)	T (deg. C)	n	ΔH (kcal)	K_b (mM^{-1})	ΔG (kcal)	$T\Delta S$ (kcal)	ΔS (e.u.)
A. *Cobalt hexammine ligand, dependence on [NaCl]*							
10	25	0.217 ± 0.012	1.24 ± 0.10	230 ± 80	−7.31 ± 0.25	8.55 ± 0.35	28.7 ± 1.2
20	25	0.198 ± 0.014	1.09 ± 0.12	145 ± 65	−7.04 ± 0.35	8.13 ± 0.47	27.3 ± 1.6
30	25	0.176 ± 0.011	0.92 ± 0.07	78 ± 14	−6.67 ± 0.11	7.59 ± 0.18	25.5 ± 0.6
40	25	0.181 ± 0.016	0.72 ± 0.05	57 ± 9	−6.49 ± 0.10	7.21 ± 0.15	24.2 ± 0.5
100	25	0.164 ± 0.017	0.29 ± 0.04	41 ± 11	−6.29 ± 0.18	6.58 ± 0.22	22.1 ± 0.7
B. *Cobalt hexammine ligand, dependence on temperature*							
10	25	0.217 ± 0.012	1.24 ± 0.10	230 ± 80	−7.31 ± 0.25	8.55 ± 0.35	28.7 ± 1.2
10	37	0.199 ± 0.006	1.47 ± 0.11	113 ± 23	−7.17 ± 0.14	8.64 ± 0.25	27.9 ± 0.8
10	50	0.236 ± 0.021	1.87 ± 0.29	280 ± 120	−8.05 ± 0.36	9.92 ± 0.65	30.7 ± 2.0
10	65	0.198 ± 0.009	2.4 ± 0.4	87 ± 30	−7.64 ± 0.28	10.0 ± 0.68	29.7 ± 2.0
C. *Spermidine ligand*							
10	25	0.199 ± 0.005	1.28 ± 0.06	140 ± 40	−7.02 ± 0.20	8.30 ± 0.26	27.8 ± 0.9

Stoichiometries (n, equivalend to $1/z$), enthalpies (ΔH), and the association constants (K_b) were obtained by regression analysis of several titration repeats, of the sort shown in Figures 2-4.

bound cation were endothermic: +1.24(±0.10) kcal for cobalt hexammine, and +1.28(±0.06) kcal for spermidine. Association constants were 230,000(±80,000) and 140,000(±40,000) M^{-1}, respectively, leading to free energies of −7.31(±0.25) and −7.02(±0.20) kcal/mol. The entropies were positive, 28.7 and 27.8 cal/mol K, overcoming the unfavorable enthalpy of binding and showing that the multivalent cation binding is entropically driven. These smal positive enthalpies and large positve entropies are found uniformly throughout this study.

Dependence on ionic strength

Figure 3 shows that cobalt hexammine binding to DNA, and subsequent DNA condensation, depend strongly on the ionic strength of the solution. Similar behavior was exhibited by spermidine (data not shown). Standard calorimetric data regression analysis yielded the stoichiometries, enthalpies, and association constants listed in Tables 1 and 2.

The number of cobalt hexammine ions bound per DNA phosphate in the first stage decreased from 0.217 to 0.164 upon increasing NaCl concentration from 10 to 100 mM (Table 1). The enthalpy of binding decreased from +1.24 to +0.29 kcal/mol, and the association constants decreased from 230,000 to 41,000 M^{-1}. Thermodynamic parameters for the second stage were determined with less accuracy, and only in the salt range between 10 and 30 mM (Table 2). Within the error of the measurements the stoichiometry of the second stage remained practically unchanged and was approximately equal to 0.07(±0.03) mol of cobalt hexammine bound per mole DNA phosphate. Similarly to the first stage, the enthalpy of binding was endothermic and decreased with increased salt concentration. Free energies and entropies of binding remained practically constant with increased salt, at −8 kcal/mol and 29 cal/mol K, respectively.

Dependence on temperature

Curves of cobalt hexammine binding at temperatures between 25 and 65 °C are shown in Figure 4. The resulting thermodynamic parameters are listed in Table 1 for the first stage and in Table 2 for the

Table 2. Thermodynamic parameters of the second stage of cobalt hexammine and spermidine interaction with pUC118 plasmid DNA

[NaCl] (mM)	T (deg. C)	n	ΔH (kcal)	K_b (mM^{-1})	ΔG (kcal)	$T\Delta S$ (kcal)	ΔS (e.u.)
A. *Cobalt hexammine ligand, dependence on [NaCl]*							
10	25	0.059 ± 0.012	0.82 ± 0.09	600 ± 160	−7.88 ± 0.18	8.70 ± 0.27	29.2 ± 0.9
20	25	0.075 ± 0.014	0.58 ± 0.06	900 ± 400	−8.12 ± 0.35	8.70 ± 0.41	29.2 ± 1.4
30	25	0.052 ± 0.009	0.31 ± 0.06	460 ± 220	−7.73 ± 0.39	8.04 ± 0.45	27.0 ± 1.5
B. *Cobalt hexammine ligand, dependence on temperature*							
10	25	0.059 ± 0.012	0.82 ± 0.09	600 ± 160	−7.88 ± 0.18	8.70 ± 0.27	29.2 ± 0.9
10	37	0.061 ± 0.007	1.45 ± 0.14	400 ± 70	−7.95 ± 0.12	9.40 ± 0.26	30.3 ± 0.8
10	50	0.080 ± 0.011	2.3 ± 0.3	1400 ± 300	−9.09 ± 0.18	11.4 ± 0.48	35.3 ± 1.5
10	65	0.081 ± 0.013	2.9 ± 0.4	1000 ± 400	−9.28 ± 0.32	12.2 ± 0.72	36.1 ± 2.1
C. *Spermidine ligand*							
10	25	0.11 ± 0.26	0.45 ± 0.08	420 ± 140	−7.67 ± 0.24	8.12 ± 0.32	27.2 ± 1.1

Data of the second peak was independently regressed against two kinds of independent binding sites model.

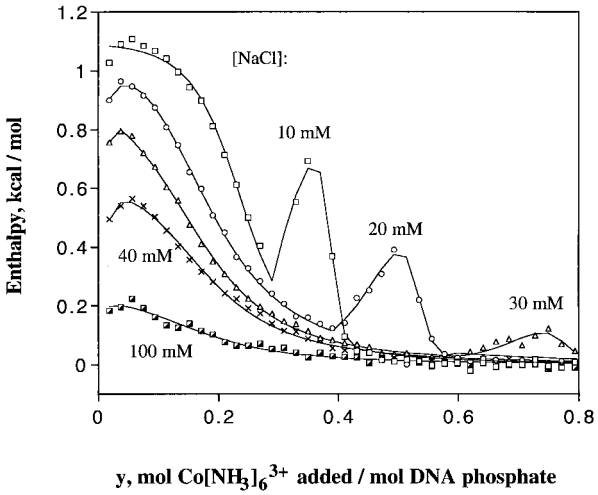

Figure 3. Isothermal titration calorimetric curves of cobalt hexammine binding to circular pUC118 DNA at various NaCl concentrations: 10 mM (□), 20 mM (○), 30 mM (△), 40 mM (×), and 100 mM (half-filled squares). Both the first binding stage, and the second aggregation stage were affected: increasing concentrations of NaCl weakened binding and delayed aggregation stage.

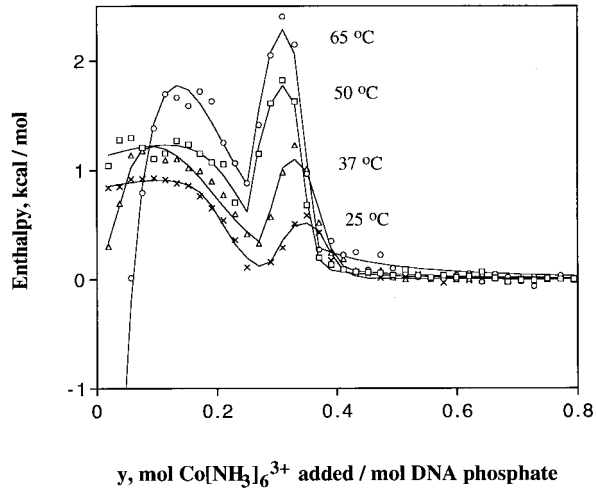

Figure 4. Isothermal titration calorimetric curves of cobalt hexammine binding to circular pUC118 DNA at various temperatures: 25 °C (×), 37 °C (△), 50 °C (□), and 65 °C (○). The enthalpy of reaction was more endothermic at higher temperatures for both the binding and aggregation stages. Two first points of the curve obtained at 65 °C were truncated in order to save space. The points were at −1.9 and −4.0 kcal/mol. Analysis yielded the initial enthalpy of −8 kcal/mol, which indicates reannealing of partially melted DNA due to stabilization of double-helical DNA by bound cobalt hexammine.

second stage. Enthalpic contributions to the binding reactions of both stages were more endothermic at higher temperatures. The stoichiometries of both binding stages remained unchanged at about 0.21 and 0.07 cobalt hexammine bound per DNA phosphate. At 65 °C a reannealing reaction of the partially melted plasmid double helix occurred after cobalt hexammine addition, as indicated by the large exothermic enthalpy (−8 kcal/mol) at the beginning of the titration. This resulted from stabilization of the DNA double helix by cobalt hexammine.

The heat capacities of first and second stage binding reactions, calculated from the linear increase of enthalpies with temperature, were also obtained. For the first stage $\Delta C_p = 29(\pm 8)$ cal/mol K, and for the second stage, 53(±15) cal/mol K.

Analysis of Binding by Electrostatic Theory

First stage of binding

To this point we have analyzed the ITC data by applying a standard, simple non-cooperative binding model. However, we know that non-specific electrostatic forces play an essential role in ionic binding reactions. Here we evaluate the relative contribution of electrostatic forces to the overall binding energetics.

Non-specific electrostatic binding of z-valent cations to DNA is determined by competition with the monovalent cations in screening the net charge of DNA. If the molar concentrations of added z-valent and monovalent cations are N_z and N_1, then the fraction of DNA phosphate charge neutralized by z-valent cations ($z\Theta$, where Θ is the number of cobalt hexammine^{3+} or spermidine^{3+} cations bound per DNA phosphate) is (Rouzina & Bloomfield, 1997):

$$z\Theta = K[\text{DNA-P}]N_z(1 - z\Theta)^z \quad (1)$$

where K is the binding canstant in molar units. This binding constant is predicted from electrostatic assumptions to equal:

$$K = \left(\frac{N_s}{N_1}\right)^z \frac{1}{N_z[\text{DNA-P}]} \quad (2)$$

where [DNA-P] is the molar concentration of DNA phosphates in solution (0.50 mM at the beginning of titration in our experiments), and N_s is the maximum counterion concentration at the DNA surface, which depends on surface charge density σ:

$$N_s = 2\pi(\sigma/e)^2 l_B \quad (3)$$

Here e is the proton charge, and l_B is the Bjerrum length:

$$l_B = e^2/\varepsilon k_B T \quad (4)$$

The dielectric constant of water is ε, k_B is the Boltzmann constant, and T is the temperature. For a long B-DNA polymer, N_s is calculated to be ≈1 M.

Thus, the binding constant is predicted to depend strongly on the concentration of monovalent salt, and weakly on the surface charge density.

If the added concentration of z-valent cations (N_z in equation (1)) is low enough to decrease significantly due to binding to DNA, then the concentration of remaining unbound z-valent cations is equal to:

$$N_{z,\text{free}} = N_z - \Theta[\text{DNA-P}] \tag{5}$$

Substituting this relation into equation (1) we obtain:

$$z\Theta = K[\text{DNA-P}](y - \Theta)(1 - z\Theta)^z \tag{6}$$

where $y = N_z/[\text{DNA-P}]$ is the ratio of added z-valent cation and DNA phosphate molar concentrations.

Let us note here the small formal difference between the standard equation of calorimetric data analysis:

$$z\Theta = K[\text{DNA-P}]N_z(1 - z\Theta), \tag{7}$$

and the electrostatic binding model, equation (1). The difference between the two models is that the calorimetric model treats each binding microreaction independently, while the electrostatic binding model (Manning, 1978; Rouzina & Bloomfield, 1996a, 1997) includes anticooperativity by raising the fraction of unneutralized DNA charge $(1 - z\Theta)$ to the zth power. This predicts that triply charged cations will bind to DNA with three times more negative free energy than singly charged cations, and that the binding constant of triply charged cations will equal the cube of the binding constant of singly charged cations.

Isothermal titration calorimetry yields the enthalpy evolved upon titration of DNA with cationic ligand:

$$H(y) = H_I \frac{\partial\Theta}{\partial y} \tag{8}$$

where $H(y)$ is the enthalpy evolved in the yth injection, and H_I is the integral enthalpy of cationic ligand binding to DNA. The derivative can be found from the analytical form of the binding isotherm, equation (6). In the limit when binding is small, $\Theta \to 0$, and:

$$\frac{\partial\Theta}{\partial y} = \frac{1}{1 + \dfrac{z}{K[\text{DNA-P}]}} \tag{9}$$

The electrostatic component of the free energy of cation binding to DNA is:

$$\Delta G = -zRT\ln(N_s/N_1) = -RT\ln K \tag{10}$$

The electrostatic free energy predicted from this equation at 10 mM NaCl salt ($N_1 = 0.01$ M), with $z = 3$ and $N_s \sim 1$ M, is -8.2 kcal/mol.

The electrostatic component of the enthalpy of cation binding to DNA can be found from:

$$\Delta H = \frac{\partial(\Delta G/T)}{\partial(1/T)} = -T^2\frac{\partial(\Delta G/T)}{\partial T} = zRT(\nu - 1) \tag{11}$$

where $\nu = 1.4$ is the experimentally determined exponent in the equation for the temperature dependence of the dielectric constant of water:

$$\varepsilon = \varepsilon^*(T^*/T)^\nu \tag{12}$$

where ε^* is the dielectric constant of water at $T^* = 298$ K. According to this relation, the predicted electrostatic enthalpy of binding is +0.71 kcal/mol. Thus, the predicted enthalpy is small and positive, opposing the binding. The contribution of entropy ($T\Delta S$) to the binding free energy would then be equal to +8.9 kcal/mol. These values agree well with the thermodynamic parameters listed in Table 1, which were obtained by applying the standard calorimetric method of data analysis.

Figure 5 compares the electrostatically modeled titration curves with those obtained experimentally by ITC. We used equations (6) and (8) to fit the cobalt hexammine binding at the NaCl concentrations in Figure 3, with K the only adjustable parameter. The integral enthalpy of binding H_I was assumed to be independent of $[Na^+]$, with a best value for all curves of 1.1(±0.1) kcal/mol. The agreement is satisfactory, especially at the early stages of titration, particularly if it is borne in mind that the fitting was carried out by varying a single parameter, the equilibrium constant. By contrast, in the conventional fitting of titration calorimetric

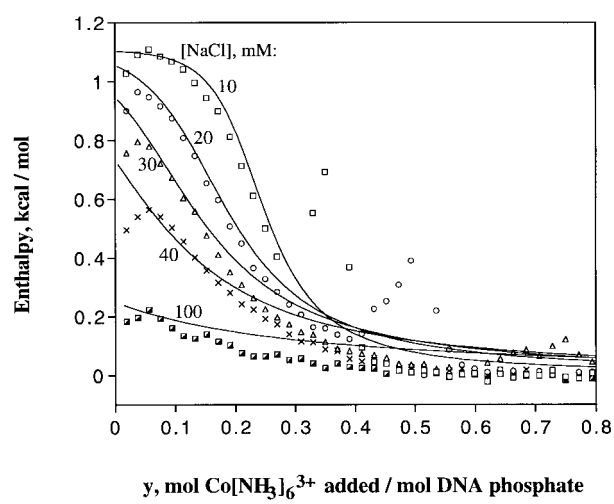

Figure 5. The curves of cobalt hexammine binding to DNA at various NaCl concentrations, simulated according to electrostatic binding model (continuous lines) as compared to the actual experimental titration data taken from Figure 3, where the meanings of the symbols are described.

Table 3. Thermodynamic parameters of cobalt hexammine and spermidine binding to pUC118 plasmid DNA in the first stage calculated by fitting binding curves, shown in Figure 5, using the electrostatic model

[NaCl] (mM)	T (deg. C)	n	ΔH (kcal)	K_b (mM^{-1})	ΔG (kcal)	$T\Delta S$ (kcal)	ΔS (e.u.)
A. *Cobalt hexammine ligand, dependence on [NaCl]*							
10	25	3	1.10 ± 0.10	1100 ± 200	−8.24 ± 0.12	9.34 ± 0.22	31.3 ± 0.7
20	25	3	1.10 ± 0.10	120 ± 30	−6.93 ± 0.17	8.03 ± 0.27	26.9 ± 0.9
30	25	3	1.10 ± 0.10	36 ± 8	−6.22 ± 0.15	7.32 ± 0.25	24.6 ± 0.8
40	25	3	1.10 ± 0.10	12 ± 2	−5.56 ± 0.10	6.66 ± 0.20	22.3 ± 0.7
100	25	3	1.10 ± 0.10	1.6 ± 0.4	−4.37 ± 0.17	5.47 ± 0.27	18.3 ± 0.9
B. *Cobalt hexammine ligand, dependence on temperature*							
10	25	3	0.95 ± 0.10	1000 ± 200	−8.19 ± 0.14	9.14 ± 0.24	30.7 ± 0.8
10	37	3	1.16 ± 0.10	800 ± 200	−8.38 ± 0.18	9.54 ± 0.28	30.8 ± 0.9
10	50	3	1.30 ± 0.1	1200 ± 200	−8.99 ± 0.12	10.29 ± 0.22	31.8 ± 0.7
10	65	3	1.80 ± 0.2	1600 ± 300	−9.60 ± 0.14	11.4 ± 0.34	33.7 ± 1.0
C. *Spermidine ligand*							
10	25	3	1.28 ± 0.06	1000 ± 200	−8.19 ± 0.14	9.14 ± 0.24	30.7 ± 0.8

data there are three variables: the enthalpy of binding, the equilibrium constant, and the stoichiometry of binding. The association constants used to generate the curves are listed in Table 3, along with the derived thermodynamic parameters. Comparing with Table 1, we see that the electrostatic method leads to significantly greater salt dependence of K, ΔG, and ΔS than does the calorimetric analysis.

From the electrostatic component of free energy (equation (10)) we can state that:

$$\Delta G/RT = -\ln K = -z\ln(N_s) + z\ln[\mathrm{Na}^+] = 3\ln[\mathrm{Na}^+] \quad (13)$$

A plot of measured $\Delta G/RT$ *versus* $\ln[\mathrm{Na}^+]$ yields a slope of 2.85, which is close to the expected value of $z = 3$ if $N_s = 1$ M. The equation of best fit is:

$$\Delta G/RT = -0.53 + 2.85\ln[\mathrm{Na}^+] \quad (14)$$

For comparison, a plot of the cobalt hexammine binding data measured by equilibrium dialysis (Plum & Bloomfield, 1988) yields a slope of 2.3. The two sets of data are very close within experimental error.

The intercept of −0.53 in equation (14) yields a value for N_s of 1.20 M. This is close to the theoretical estimate of $N_s \approx 1$ M. To achieve best agreement with the equilibrium dialysis data, the intercept should changed to −1.07, which would correspond to $N_s = 1.43$ M. We should note that the theoretical estimate for N_s contains an uncertain factor, close to unity, due to the ill-defined distance of closest approach of the cation to the DNA surface (Rouzina & Bloomfield, 1996a,b, 1997). Another part of the discrepancy is presumably due to non-electrostatic components of the binding.

Second stage of binding and condensation

Assuming that the second peak in the ITC curves is due to DNA condensation (an assumption made plausible by the development of visible turbidity only after the peak develops) we can find the concentratians of cobalt hexammine that cause DNA condensation at each salt concentration. Figure 6 shows the dependence of the critical cobalt hexammine concentration (at the midpoint of DNA condensation) on [Na$^+$]. Our calorimetric data are consistent with data obtained by light scattering and osmotic stress measurements (Rau & Parsegian, 1992a; Widom & Baldwin, 1980; Wilson & Bloomfield, 1979). The critical [cobalt hexammine] appears to be practically independent of the DNA concentration used in the experiment. The difference in [cobalt hexammine] between the beginning and end of the DNA condensation transition as measured by ITC is also provided for comparison in Figure 6.

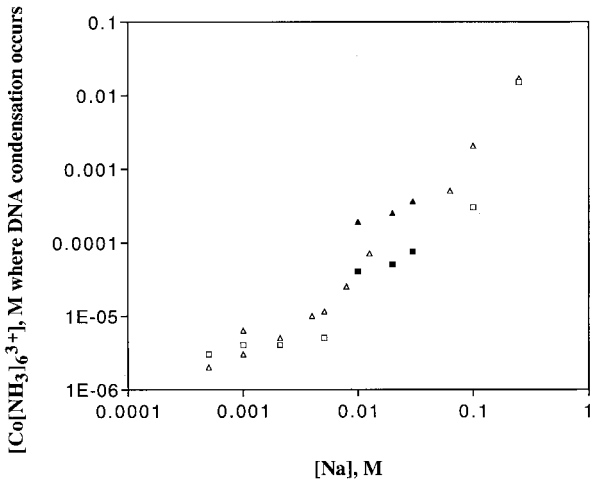

Figure 6. Dependence of the critical cobalt hexammine concentration for DNA condensation on salt. Comparison of our calorimetric data (filled symbols) with light scattering and osmotic stress data obtained by other researchers (open symbols). Triangles represent cobalt hexammine concentrations where DNA condensation midpoints occur, squares represent the differences between cobalt hexammine concentrations where DNA condensation begins and ends.

Using the binding constants determined by fitting calorimetric data with the electrostatic model, we can calculate the critical fraction of DNA phosphates neutralized by cobalt hexammine, $z\Theta_{cr}$, at the critical [cobalt hexammine] needed to cause DNA condensation. At 10 mM NaCl we get $z\Theta_{cr} = 0.70$, at 20 mM NaCl $z\Theta_{cr} = 0.64$, and at 30 mM NaCl $z\Theta_{cr} = 0.60$. Thus, the fraction of charge that must be neutralized by cobalt hexammine in order for DNA to condense is fairly independent of $[Na^+]$, and is approximately equal to two-thirds. This value of two-thirds was also obtained from the standard non-cooperative binding model, making the result self-consistent and confirming the conclusion.

For DNA condensation with spermidine, the second peak occurs at much higher ligand concentration (at 10 mM NaCl the peak maximum was at 0.16 mM for cobalt hexammine and 0.39 mM for spermidine). From the fitted K_b value for spermidine in Table 3 we determine that $z\Theta_{cr} = 0.87$ at 10 mM, NaCl, which is significantly greater than 0.70 for cobalt hexammine.

Discussion

Thermodynamics from ITC

We have described the thermodynamics of two consecutive processes in the course of a single ITC experiment. Initially, cationic ligand, cobalt hexammine or spermidine, bound to negatively charged DNA. After reaching a critical ligand concentration, DNA condensation occurred. The thermodynamic parameters for both processes were very similar. This suggests that these parameters are assignable to the same process, ligand binding, which occurs during both stages. During the second stage, DNA condenses and DNA-DNA interactions occur. We cannot assign any thermodynamic parameters to these interactions.

In a study that obtained similar results by different techniques, two stages of spermine^{4+} binding to DNA were observed using fast reaction kinetics methods (Pörschke, 1984). During the first or induction period, spermine molecules bound to DNA but Θ remained below the critical or threshold value. In a slower process that apparently corresponds to our second stage, the remaining spermine bound and DNA condensed. Two-step behavior was also observed in a study of the binding of singly charged cationic lipid cetyltrimethylammonium bromide to DNA by ITC (Spink & Chaires, 1997). During the first phase lipid cation bound to DNA phosphate, and during the second phase the hydrophobic tails of the lipid cooperatively interacted with each other.

Our calorimetry experiments are in good agreement with equilibrium dialysis experiments on the salt dependence of cobalt hexammine binding to DNA (Plum & Bloomfield, 1988), and with the finding that the initial stages of cobalt hexammine and spermidine binding to DNA are indistinguishable (Braunlin *et al.*, 1982; Plum & Bloomfield, 1988). They are also in good agreement (see below) with osmotic stress measurements of excess cobalt hexammine binding accompanying spontaneous assembly of DNA molecules into hexagonal arrays (Rau & Parsegian, 1992a).

ITC showed that both the first and second stages of cobalt hexammine or spermidine binding were entropically driven and accompanied by a relatively small unfavorable change in enthalpy. Heat capacity changes for both processes were positive. It is noteworthy that ITC is able to provide detailed information about an entropically driven process by measuring relatively small enthalpic changes that oppose the binding reaction. Such cases are unusual in calorimetry. For comparison, binding of a single-stranded binding protein to a single-stranded DNA evolves large exothermic enthalpy, and is associated with negative heat capacity change (Kozlov & Lohman, 1998).

Electrostatic theory of cation binding and DNA condensation

The thermodynamics of binding of cationic ligands to DNA are generally well explained by the electrostatic binding model. This model accurately predicts the free energy of association and provides an estimate of the small positive contribution of electrostatics to the binding enthalpy, which arises from the temperature dependence of the dielectric constant of water. The electrostatic model not only correctly predicts the titration curve of trivalent cationic ligand binding to DNA, but also provides an explanation for the strong dependence on monovalent salt concentration of the association constant by requiring that $K \sim [Na^+]^{-z}$ (Manning, 1978; Rouzina & Bloomfield, 1996a, 1997).

However, the DNA condensing capabilities of cobalt hexammine and spermidine were confirmed to be quite different as concluded earlier by equilibrium dialysis and NMR experiments (Braunlin *et al.*, 1982, 1986, 1987).

It has been proposed that one of the favorable contributions that drives DNA condensation process is counterion-mediated attraction, of which two forms have been suggested: a self-organizing surface lattice (Rouzina & Bloomfield, 1996c) and fluctuations in the diffuse ion atomosphere (Gronbech-Jensen *et al.*, 1997; Oosawa, 1968). The present study provides new arguments in favor of a non-specific electrostatic counterion correlation mechanism of DNA attraction, since ΔH is small and positive, rather than large and negative as would likely be the case if specific site binding of condensing ligands were important. The attraction increases with the increasing number of multivalent counterions bound to the DNA condensate. It is therefore energetically favorable to bind the maximal number of cobalt hexammine counterions allowed by the neutralization condition. At the moment of condensation an additional fraction of

DNA charge, screened with monovalent Na^+ cations, should be replaced by cobalt hexammine. This increase in cobalt hexammine binding upon DNA condensation is expressed through the second peak of endothermic enthalpy. Such increase in binding during DNA condensation was also observed in an osmotic stress study (Rau & Parsegian, 1992a). In 0.25 M NaCl, a considerably higher salt concentration than we used in this study, 17 mM cobalt hexammine was required for spontaneous assembly of DNA bundles. This was accompanied by additional binding of 0.20 cobalt hexammine per base-pair, corresponding to neutralization of 0.30 of the DNA charge. This is in excellent agreement with the additional charge neutralization that we observe in the second stage of cobalt hexammine binding and that has been observed in solution studies of DNA condensation (Widom & Baldwin, 1980; Wilson & Bloomfield, 1979).

DNA condensation was entropically driven in a similar fashion to cobalt hexammine binding. A similar conclusion was reached in the thermodynamic analysis of the osmotic stress-induced condensation of DNA in the presence of multivalent cations (Leikin *et al.*, 1991; Rau & Parsegian, 1992a,b). In those studies it was argued that the source for the entropy increase accompanying DNA condensation must be the change in entropy of water induced by the approaching DNA, molecules, and thus that the hydration force is the source of attraction between DNA molecules. However, the hydration force and electrostatic mechanisms may be indistinguishable in an aqueous environment, since the orientation of the water dipoles by ions and charged surfaces (manifested in the temperature-dependent dielectric constant of water) also leads to a positive entropic contribution.

A comparison of DNA condensation by cobalt hexammine and spermidine provides another piece of evidence in favor of the electrostatic DNA condensation model. According to electrostatic arguments there should be no difference in how these cations bind to DNA, an expectation confirmed both by the first stage of our ITC curves and by equilibrium dialysis experiments (Braunlin *et al.*, 1982; Plum & Bloomfield, 1988). However, electrostatic correlations should be more pronounced, and attraction stronger between charged DNA surfaces, when counterion charge is more compact (Rouzina & Bloomfield, 1996c). Since cobalt hexammine is more compact than spermidine, this explains the experimental result that it is also a more effective DNA condensing agent (Widom & Baldwin, 1980).

Aspects not explained by electrostatics

The binding curves shown in Figure 5 were well described by polyelectrolyte binding isotherms only for moderate degrees of binding, when $z\Theta < 0.5$. At near saturating levels of binding, the measured enthalpy was systematically lower than predicted. There could be at least two reasons for this discrepancy. First, the enthalpy of binding may be not identical for the first binding sites, when there is no interaction between neighboring ligands, and near the end of binding when such interaction is inevitable. Second, the electrostatic correlation between counterion becomes progressively stronger for multivalent ions as they accumulate at the DNA surface and eventually lead to DNA condensation (Rouzina & Bloomfield, 1996c); this increased correlation should be accompanied by a more negative correlation energy. It should be remembered that the curves were fitted with a single value of the enthalpy of cobalt hexammime binding, 1.1 kcal/mol, consistent with the expectation from polyelectrolyte theory that the enthalpy should be small and independent of salt.

The enthalpy of binding depended strongly on temperature, yielding a positive heat capacity change of 20-50 cal/mol K, behavior inexplicable by a simple polyelectrolyte theory. The predicted electrostatic heat capacity, $\Delta C_p^{el} = zR(\nu - 1) = 2.4$ cal/mol K, can account only about 10 % of the observed value. The rest of the heat capacity change may be explained, at least in part, by the burial of the polar surfaces of DNA and ligand upon binding. Such burial of polar surfaces in aqueous solutions typically has $\Delta C_p = 0.14(\pm 0.04)$ cal/mol K Å^2 (Spolar *et al.*, 1992; Spolar & Record, 1994).

The small positive enthalpy of cobalt hexammine binding might also be explained chemically rather than electrostatically. The enthalpy of dissolution of inorganic anhydrous ammonium phosphate in water is equal to −0.75 kcal/mol phosphate (calculated from data in the *CRC Handbook of Chemistry and Physics*). Therefore, the enthalpy of crystallization would be +0.75 kcal/mol, similar to the value of +1.1 kcal/mol cobalt hexammine bound to DNA. Thus, there might be similarities between how the ionic hydrogen bonds form in inorganic ammonium phosphate crystals, and how DNA phosphates interact with amines in spermidine and cobalt hexammine. Following this analogy, water may be released from the immediate hydrational environment of DNA phosphates and multivalent counterions upon DNA condensation.

Structural and energetic model of binding and DNA condensation

Figure 7 summarizes our proposed model for cobalt hexammine and spermidine binding to double-helical DNA, and for DNA condensation as the result of the binding. During the first stage, trivalent cations bind to DNA due to attractive electrostatic forces. Ammonium groups on one side of cobalt hexammine cation may form weak, short-lived hydrogen bonds with O6 in phosphates, N7 atoms in guanine residues, or some other sites, as seen in DNA-cobalt hexammine cocrystal structures (Neidle, 1999). Hydrogen bond formation may explain why the enthalpy of binding is not

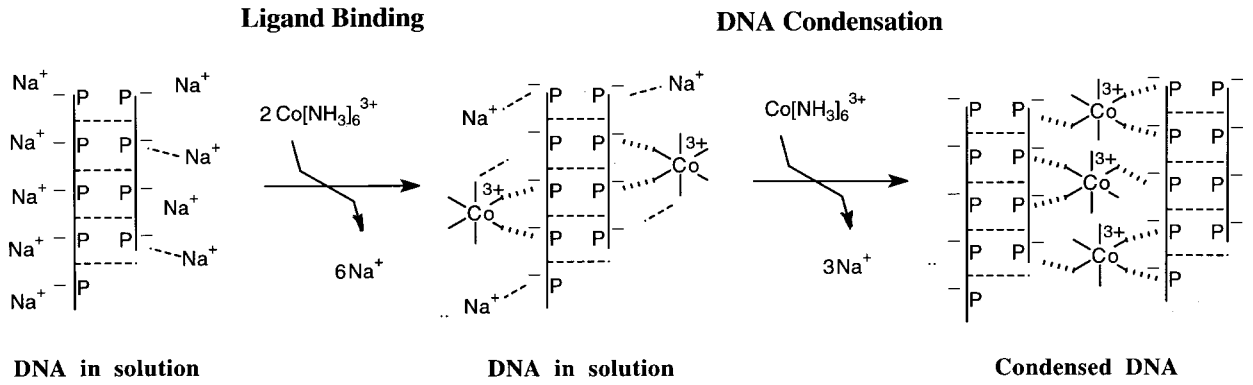

Figure 7. Proposed two-stage mechanism to explain the isothermal calorimetry results: cobalt hexammine binding to DNA in the first stage and DNA condensation in the second stage. Bound counterions are delocalized or bound by short-lived hydrogen bonds. Stoichiometries of binding for each stage are indicated. The electrostatic model accounts for most of the energetics.

exactly 0.71 kcal/mol, as expected from electrostatic assumptions. Ammonium groups on the other side of the cobalt hexammine cation remain exposed to aqueous solution throughout the first stage.

After reaching some critical binding value Θ_{cr}, the partially counterion-saturated DNA begins to bind to another such partially saturated DNA double helix, beginning the second stage observed in the second peak of the ITC curves. Attraction of apposed DNA surfaces is driven largely by counterion correlation (Rouzina & Bloomfield, 1996c), causing additional trivalent cation binding and displacement of non-specifically bound sodium cations. Additional hydrogen bonds may form between the solution side of cobalt hexammine ammonium groups and another nearby DNA double helix. At the end of the second stage DNA is fully saturated by cobalt hexammine cations and is electrically neutral. In a condensed phase, DNA slowly aggregates and precipitates from aqueous solution under the relatively high concentrations used in the ITC experiments.

Materials and Methods

Isolation and purification of pUC118 plasmid DNA

Escherichia coli strain DHP5-α with pUC118 plasmid was obtained from Dr Anath Das, University of Minnesota; it is available from Worthington Biochemical Corporation (Lakewood, NJ). Cells were grown in six litres of LB medium containing ampicillin. Plasmid was isolated using Qiagen (Valencia, CA) Endo Free Giga plasmid isolation kit. For comparison between linear and circular molecules, we cut 10 mg of the plasmid at its single *Sma*I restriction site with 10,000 units of enzyme (Fermentas AB, Vilnius, Lithuania) producing blunt-ended molecules with three GC repeats. No significant difference was found between circular and linear DNA (Figure 2), so most experiments were carried out with circular plasmid which was easier to prepare on a large scale.

Chemicals

Cobaltic(III) hexammine trichloride (cobalt hexammine) was obtained from Kodak, and spermidine trihydrochloride was obtained from Sigma. Both were used without further purification.

Isothermal titration calorimetry of ligand binding

Isothermal titration calorimetry (ITC) was performed with a Microcal (Northampton, MA) MCS calorimeter at 25.0 °C unless otherwise specified. The cell volume was 1.3438 ml. The calorimeter was checked using the Tris base reaction with HCl, for which $\Delta H = -11.38$ kcal/mol acid neutralization.

Two milliliters of pUC118 DNA solution in 10 mM NaCl (unless otherwise specified) (pH 6.8-6.9) with no buffer, were added to the calorimeter cell. The concentration of the DNA phosphate groups in the cell was 0.50 mM at the beginning of titration. Cobalt hexammine (2.0 mM), or spermidine (4.0 mM), at the same pH as in the cell, were injected in 40 portions of 6.25 μl with a 250 μl injection syringe, at three minute intervals.

Figure 1 shows two representative non-integrated titration curves. The upper curve was obtained by titrating DNA (0.5 mM phosphate) with 2 mM cobalt hexammine in the presence of 10 mM NaCl. The lower curve was obtained by titrating 2 mM cobalt hexammine into the cell without the DNA in the presence of 10 mM NaCl. The lower curve shows the heats of cobalt hexammine dilution, and the upper curve shows the heats resulting from both the dilution effect and the binding reactions. The peaks in both curves were integrated and the heats of dilution were subtracted, yielding an integrated curve of the sort shown in Figures 2-4. The small heat of dilution shows that the peaks in these Figures arise from binding, not from ligand dilution.

Note that the baseline stability is relatively good, with the drift of less than 0.1 mcal/second per hour. The greatest baseline instability occurs during the second stage of binding, i.e. during DNA condensation. The short-term noise of the baseline was less than ±0.005 μcal/second per minute.

Standard analysis of integrated titration calorimetry curves

Experiments were repeated at least twice, and regressed independently. The standard errors shown in Tables 1 and 2 were obtained from analysis of several repeats, and are usually greater than the regression errors given by fitting a single titration curve.

Two separate models were regressed against the ITC data, using Microcal Origin software in the standard way described in the manual (Microcal, 1993): (1) a single set of identical binding sites; (2) two sets of independent binding sites. The regression parameters included the integral enthalpies of binding, stoichiometries of binding, and association constants (K_b) for each set of sites. Formulae used in data analysis for the model of a single set of binding sites may be found in the work by Merabet & Ackers (1995), and for the model of two sets of independent sites in the work by Lin *et al.* (1991). The software takes into account incomplete binding of ligand. For example, if we compare the enthalpy of binding in Figure 2 (which appears to be 1.1 kcal/mol) with the value in Table 1 (1.24 kcal/mol) there seems to be a discrepancy. The value in Table 1 is correct; the discrepancy appears because binding is not complete and only approximately 90% of added cobalt hexammine during the first injection actually binds to DNA.

Most of the ITC curves had two seemingly independent stages of binding (e.g. see Figure 2). In those cases the data were separated into two sets by eye and independent regression analyses for each set were carried out. Both the single set of identical binding sites and the two sets of independent binding sites models were tested, and the regression parameters tabulated for the best fits.

Free energies were calculated from the association constants using the equation $\Delta G^\circ = -RT \ln K_b$. The entropies were calculated using the equation $\Delta S = (\Delta H - \Delta G)/T$.

Simulation of ITC curves for electrostatic binding model

The MathPad program (http://pubpages.unh.edu/~mwidholm/MathPad/) was used to simulate ITC curves according to the electrostatic binding model The theory and application of this model are described in Results.

Acknowledgements

This research was supported in part by NIH research grant GM28093. We are grateful to Professor Leonard Banaszak for use of the isothermal titration.

References

Bloomfield, V. A. (1996). DNA condensation. *Curr. Opin. Struct. Biol.* **6**, 334-341.

Bloomfield, V. A. (1998). DNA condensation by multivalent cations. *Biopolymers,* **44**, 269-282.

Braunlin, W. H., Strick, T. J. & Record, M. T., Jr (1982). Equilibrium dialysis studies of polyamine binding to DNA. *Biopolymers,* **21**, 1301-1314.

Braunlin, W. H., Anderson, C. F. & Record, M. T., Jr (1986). ^{23}Na-NMR investigations of counterion exchange reactions of helical DNA. *Biopolymers,* **25**, 205-214.

Braunlin, W. H., Anderson, C. F. & Record, M. T., Jr (1987). Competitive interactions of $Co(NH_3)_6^{3+}$ and Na^+ with helical *B*-DNA probed by ^{59}Co and ^{23}Na NMR. *Biochemistry,* **26**, 7724-7731.

Gronbech-Jensen, N., Mashl, R. J., Bruninsma, R. F. & Gelbart, W. M. (1997). Counterion-induced attraction between rigid polyelectrolytes. *Phys. Rev. Letters,* **78**, 2477-2480.

Kozlov, A. G. & Lohman, T. M. (1998). Calorimetric studies of *E. coli* SSB protein-single stranded DNA interactions. Effects of monovalent salts on binding enthalpy. *J. Mol. Biol.* **278**, 999-1014.

Leikin, S., Rau, D. C. & Parsegian, V. A. (1991). Measured entropy adenthalpy of hydration as a function of distance between DNA double helices. *Phys. Rev. ser. A,* **44**, 5272-5278.

Lin, L.-N., Mason, A. B., Woodworth, R. C. & Brandts, J. F. (1991). Calorimetric studies of the binding of ferric ions to ovotransferrin and interactions between binding sites. *Biochemistry,* **30**, 11660-11669.

Manning, G. S. (1978). The molecular theory of polyelectrolyte solutions with applications to the electrostatic properties of polynucleotides. *Quart. Rev. Biophys.* **11**, 179-246.

Merabet, E. & Ackers, G. (1995). Calorimetric analysis of λ repressor binding to DNA operator sites. *Biochemistry,* **34**, 8554-8563.

Microcal Inc., (1993). ITC data analysis in Origin Version 2.9.

Neidle, S. (1999). *Oxford Handbook of Nucleic Acid Structure*, p. 136, Oxford University Press, Oxford.

Oosawa, F. (1968). Interaction between parallel rodlike macroions. *Biopolymers,* **6**, 1633-1647.

Pelta, J., Livolant, F. & Sikorav, J. L. (1996). DNA aggregation induced by polyamines and cobalt hexamine. *J. Biol. Chem.* **271**, 5656-5662.

Plum, G. E. & Bloomfield, V. A. (1988). Equilibrium dialysis study of binding of hexammine cobalt(III) to DNA. *Biopolymers,* **27**, 1045-1051.

Pörschke, D. (1984). Dynamics of DNA condensation. *Biochemistry,* **23**, 4821-4828.

Raspaud, E., Delacruz, M. O., Sikorav, J. L. & Livolant, F. (1998). Precipitation of DNA by polyamines - a polyelectrolyte behavior. *Biophys. J.* **74**, 381-393.

Raspaud, E., Chaperon, I., Leforestier, A. & Livolant, F. (1999). Spermine-induced aggregation of DNA, nucleosome, and chromatin. *Biophys. J.* **77**, in the press.

Rau, D. C. & Parsegian, V. A. (1992a). Direct measurement of the intermolecular forces between counterion-condensed DNA double helices. Evidence for long range attractive hydration forces. *Biophys. J.* **61**, 246-259.

Rau, D. C. & Parsegian, V. A. (1992b). Direct measurement of temperature-dependent solvation forces between DNA double helices. *Biophys. J.* **61**, 260-271.

Ross, P. D. & Shapiro, J. T. (1974). Heat of interaction of DNA with polylysine, spermine, and Mg^{++}. *Biopolymers,* **13**, 415-416.

Rouzina, I. & Bloomfield, V. A. (1996a). Competitive electrostatic binding of charged ligands to polyelectrolytes: planar and cylindrical geometries. *J. Phys. Chem.* **100**, 4292-4304.

Rouzina, I. & Bloomfield, V. A. (1996). Influence of ligand spatial organization on competitive electrostatic binding to DNA. *J. Phys. Chem.* **100**, 4305-4313.

Rouzina, I. & Bloomfield, V. A. (1996). Macroion attraction due to electrostatic correlation between screening counterions. 1. Mobile surface-adsorbed ions and diffuse ion cloud. *J. Phys. Chem.* **100**, 9977-9989.

Rouzina, I. & Bloomfield, V. A. (1997). Competitive electrostatic binding of charged ligands to polyelectrolytes: practical approach using the non-linear Poisson-Boltzman equation. *Biophys. Chem.* **64**, 139-155.

Sikorav, J. L., Pelta, J. & Livolant, F. (1994). A liquid crystalline phase in spermidine-condensed DNA. *Biophys. J.* **67**, 1387-1392.

Spink, C. H. & Chaires, J. B. (1997). Thermodynamics of the binding of a cationic lipid to DNA. *J. Amer. Chem. Soc.* **119**, 10920-10928.

Spolar, R. & Record, M. T., Jr (1994). Coupling of local folding to site-specific binding of proteins to DNA. *Science,* **263**, 777-784.

Spolar, R. S., Livingstone, J. R. & Record, M. T., Jr (1992). Use of liquid hydrocarbon and amide transfer data to estimate contributions to thermodynamic functions of protein folding from the removal of nonpolar and polar surface from water. *Biochemistry,* **31**, 3947-3955.

Widom, J. & Baldwin, R. L. (1980). Cation-induced toroidal condensation of DNA: studies with $Co(NH_3)_6^{3+}$. *J. Mol. Biol.* **144**, 431-453.

Widom, J. & Baldwin, R. L. (1983). Monomolecular condensation of λ-DNA induced by cobalt hexammine. *Biopolymers,* **22**, 1595-1620.

Wilson, R. W. & Bloomfield, V. A. (1979). Counterion-induced condensation of deoxyribonucleic acid. A light-scattering study. *Biochemistry,* **18**, 2192-2196.

Edited by I. Tinoco

(Received 7 September 1999; received in revised form 15 December 1999; accepted 15 December 1999)